NUMERICAL MODELLING OF IN-PLANE BEHAVIOUR OF ADOBE WALLS

NICOLA TARQUE
PhD student
Catholic University of Peru
ROSE School-IUSS
Pavia-Italy

GUIDO CAMATA
Assistant Professor
University G. D'Annunzio
Pescara-Italy

ENRICO ESPACONE
Full Professor
University G. D'Annunzio
Pescara-Italy

HUMBERTO VARUM
Associate Professor
University of Aveiro
Aveiro-Portugal

MARCIAL BLONDET
Full Professor
Catholic University of Peru
Lima-Peru

SUMMARY

Some tests for material characterization of adobe blocks and adobe masonry have been carried out in universities and laboratories around the world. However, the number of tests is quite limited in comparison with those carried out with other structural materials, such as masonry or reinforced concrete, and even those tests just refers to elastic properties. The results of adobe tests (*i.e.* compression strength, elasticity modulus, shear strength, etc.), as well as the results of cyclic and dynamic tests on adobe masonry components and small buildings show that the mechanical properties of adobe masonry and the seismic performance of adobe constructions highly depend on the type of soil used for the production of units and mortar. Basic properties, such as elasticity modulus, can have significant variation from one soil type to another.

The state-of-the-art for the numerical modelling of unreinforced masonry point to three main approaches: macro-modelling, simplified micro-modelling and detailed micro-modelling. In all three approaches, the use of elastic and inelastic parameters is required. For adobe masonry, the lack of knowledge concerning some of the material properties makes numerical modelling more difficult.

In the proposed work, the mechanical properties of the typical adobe masonry in Peru have been calibrated based on a cyclic in-plane test carried out on an adobe wall at the Catholic University of Peru (PUCP). The mechanical parameters calibration and the modelling results of the in-plane behaviour of the adobe wall are presented. Macro-modelling and simplified micro-modelling strategies are used in finite element software with an implicit solution strategy. The results of this work represent the first step for the numerical modelling of the seismic behaviour of adobe constructions.

1. INTRODUCTION

Masonry is a composite material formed by units (bricks) and joints (mortar). Each of masonry constituents has its own material properties. Mortar is normally much weaker and softer than the bricks. However, masonry failure may involve crushing and tensile fracturing of masonry units and fracturing of masonry joints [14].

In the case of adobe structures, the bricks and mortar are made of similar materials, mainly soil. Therefore, allowing the composite to behave further as a homogeneous material. For this reason, the cracking pattern in adobe walls may not distinguish completely between blocks and mortars (Figure 1).

Since adobe walls have very low tensile strength, the cracks typically initiate in zones subjected to higher tensile stress, such as corners of doors and windows. Usually, vertical cracks start at the intersection of the façade with the perpendicular walls and create a physical separation between them; besides, and horizontal crack is formed close to the base of the façade allowing it to overturn. The typical crack pattern due to in-plane shear forces is X-diagonal shape (Figure 1). According to Webster [17], these kinds of cracks are not particularly serious unless the relative displacement across them becomes large, which triggers the overturning of the small wall blocks

formed by the cracks. Horizontal cracks may also be triggered by in-plane loading. The latter cracks are related to sliding failure modes.

Figure 1.- Typical in-plane damage in adobe walls.

2. EXPERIMENTAL TESTS ON ADOBE WALLS

Blondet *et al*. [4] carried out a displacement controlled cyclic test (push-pull) on a typical adobe wall at the Catholic University of Peru to analyze the cyclic response and the damage pattern evolution due to in-plane forces. The wall had an I-shape configuration (Figure 2), where the main longitudinal wall (with a central window opening) had 3.06 m length, 1.93 m height and a thickness of 0.30 m. Besides, this wall had two transverse walls of 2.48 m lengths to simulate the influence of connection to transversal walls common in typical buildings. The specimen was built over a reinforced concrete foundation beam. At the top of the adobe wall a reinforced concrete ring beam was built, providing the gravity loading corresponding to the roof of a typical dwelling and guarantying a more uniform distribution of the horizontal load in the wall. The horizontal cyclic loading imposed corresponds to a series of cycles with maximum displacement at the top of the wall of 1, 2, 5, 10 and 20 mm, which corresponds to 0.052%, 0.10%, 0.26%, 0.51% and 1.02% of drift, respectively. Each displacement cycle was repeated twice. During the test, the majority of the cracks followed a diagonal pattern, starting at the opening corners. Beyond the 0.52% of drift, a clear reduction of the lateral strength was observed due to the formation of large cracks in the walls. For this reason, it was decided to consider the last limit state in the test related to 0.52% of drift [15].

Figure 3 shows the final damage pattern of the adobe wall after the cyclic test. The cracks observed at the end of the cycle of 0.052% drift are marked in blue; at 0.10% drift in red; at 0.26% drift in green; and, for drift values greater than 0.51% in black.

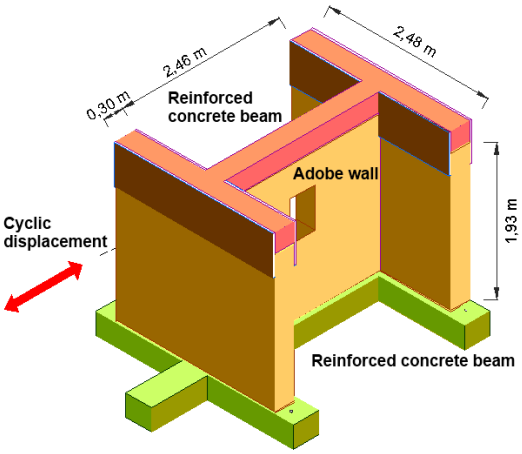

Figure 2.- Scheme of the tested wall [4].

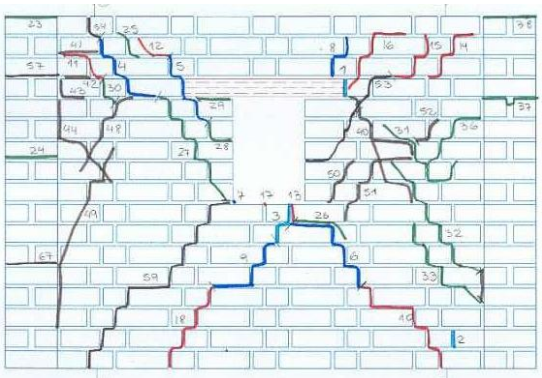

Figure 3.- Damage pattern evolution during the cyclic test [4].

This paper presents the results obtained with three different numerical models developed to represent the experimental test results. The models are developed in two finite element codes: Midas FEA [9] and Abaqus/Standard [1].

3. MODELS FOR MASONRY

Past researches have shown that failure analysis of masonry structures can be successfully described using modelling techniques usually applied to concrete mechanics [7]. According to Lourenço [8], the numerical modelling of masonry can be represented by the micro-modelling of each of its components or by macro-modelling assuming the masonry to be homogeneous. Depending on the level of accuracy, the following strategies can be used (Figure 4):

- detailed-micro modelling. Units and mortar joints are represented by continuum elements, where the unit-mortar interface is represented by discontinuous elements [2][12];
- simplified micro-modelling. The expanded units are represented by continuum elements, where the behaviour of the mortar joints and unit-mortar interface is lumped in discontinuous elements [3][10];
- macro-modelling. Units, mortar and unit-mortar interface are smeared out in the continuum and the masonry is treated as an isotropic material.

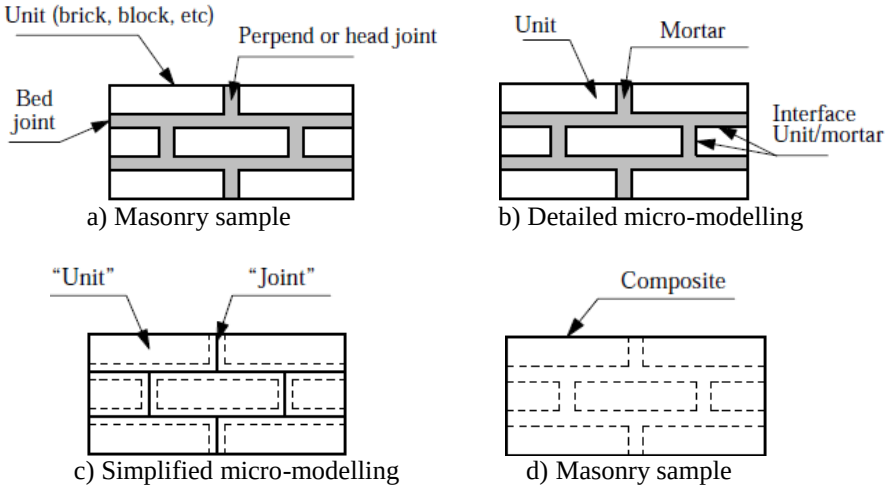

Figure 4.- Modelling strategies for masonry structures [8].

The first two approaches are computationally intensive for the analysis of large masonry structures; however, it can be an important research tool in comparison with the costly and often time-consuming laboratory experiments [6].

Lourenço [8] developed a new composite interface model for the masonry (Figure 5), capable of representing the typical failure modes as cracking of the joints, sliding along the bed or head joints at low values of normal stress, cracking of the units in direct tension, diagonal tensile cracking of the units at values of normal stress sufficient to develop friction in the joints, and splitting of the units in tension. The calibration and validation of the proposed model were based on the masonry tests carried out in Netherlands by CUR [5], Raijmakers and Vermeltfoort [11] and Vermeltfoort and Raijmakers [16][15].

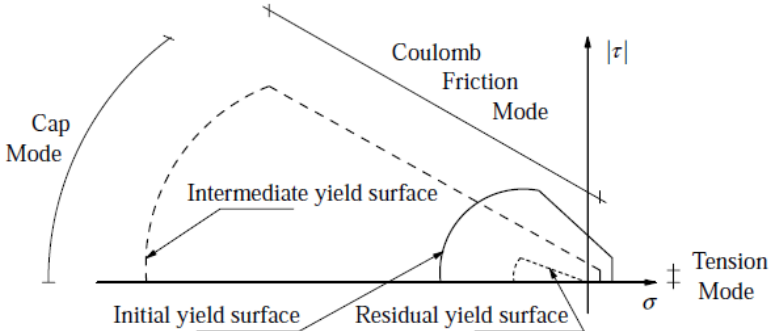

Figure 5.- Constitutive model proposed by Lourenço [8].

The objective of the model proposed by Lourenço [8] is to concentrate all the damage in the weak joints and in the potential pure tensile cracks placed vertically in the middle of each brick. This composite interface model involves the tension, shear and compression failure to represent the inelastic behaviour of the masonry, each of them associated with a hardening/softening rule. A tension cut-off it is taken for tension failure. For the shear failure, the softening process is given by the degradation of the cohesion in Coulomb friction models [10][13]. For the compression failure, Lourenço developed a suitable cap model. Since the masonry joints have extremely low dilatancy (almost zero), the model was formulated in the context of non-associated plasticity.

3.1. MIDAS FEA

A constitutive model following the same principles of the one proposed by Lourenço [8] is developed in the FE code Midas FEA. The interface elements are used to model the discrete cracks in materials or relative movements at the boundaries of model components. This interface material model called *Composite Interface model* is appropriate to simulate fracture, frictional slip as well as crushing along material interfaces, for instance at joints in masonry.

With Midas FEA it is even possible to create numerical models using a macro-modelling approach. In this case a smeared crack model (especially the *total strain model*) is used, where it is assumed that cracks are scattered and distributed along the entire surfaces of the elements. The total strain model is easy to understand since the model uses only one stress-strain relationship for tensile behaviour including cracks and one for compressive behaviour (Figure 6).

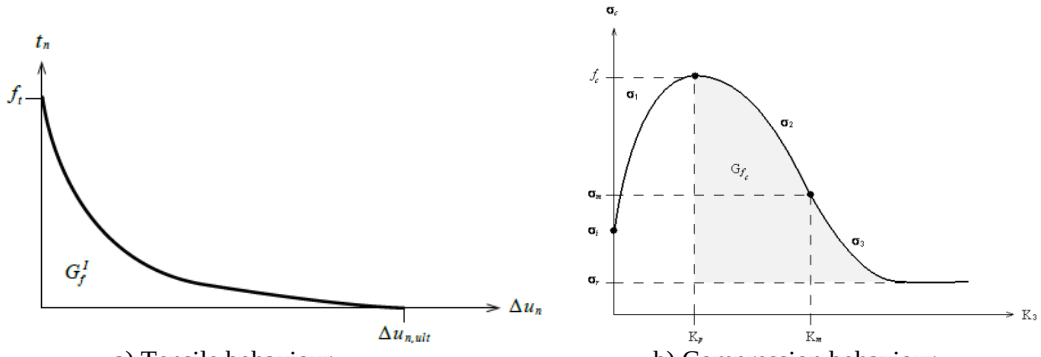

a) Tensile behaviour b) Compression behaviour

Figure 6.- Plastic behaviour of quasi-brittle materials under tension and compression loads [9].

3.2. ABAQUS

ABAQUS does not have a specific constitutive model for masonry structures, but the ones given for concrete elements and other quasi-brittle materials could be properly used to model the masonry, for example, the *concrete damage plasticity model*, where the material is characterized for tensile cracking or compressive crushing. Even, damage and stiffness recovery factors in compression and tension could be specified (Figure 7).

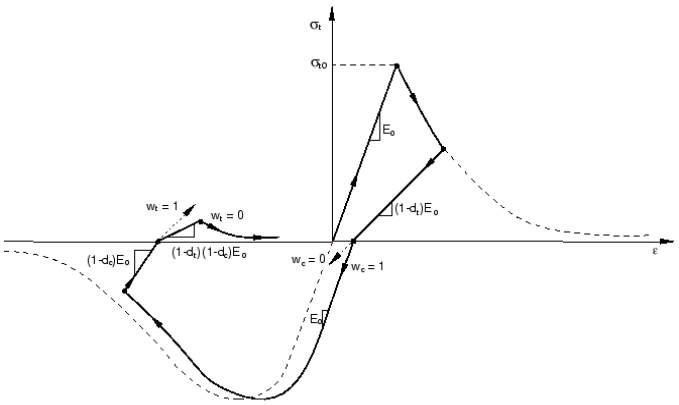

Figure 7.- Uniaxial load cycle (tension-compression-tension) [1].

4. NUMERICAL ANALYSES

The adobe wall tested by Blondet *et al.* [4] is modelled using two different constitutive models in Midas FEA (*combined interface model* with solid elements and *total strain model* with shell elements) and one constitutive model in Abaqus/Standard (*concrete damage plasticity* with shell elements). As said previously, a complete database of material properties of the adobe typically used in Peru is not available; the few data refer just to compression strength and elastic properties (*e.g.* module of elasticity) and no data is available for the inelastic properties such as fracture energy values for compression and tension. For this reason there are large uncertainties. A viable solution can be pursuing through the calibration of the unknown parameters using the experimental tests on the wall tested.

The configurations of the numerical models in Midas FEA and Abaqus/Standard are showed in Figure 8. The models include the reinforced concrete beams (at the top and at the base), the adobe walls and the timber lintel. The base is fully fixed. Since the test was displacement controlled, in the numerical model a monotonic top-displacement equal to 10 mm is applied at one vertical edge of the top concrete beam. Since the test was cyclic, further developments of these models will include the effect of cyclic loads and the analysis of stiffness recovery and damage factors for unloading.

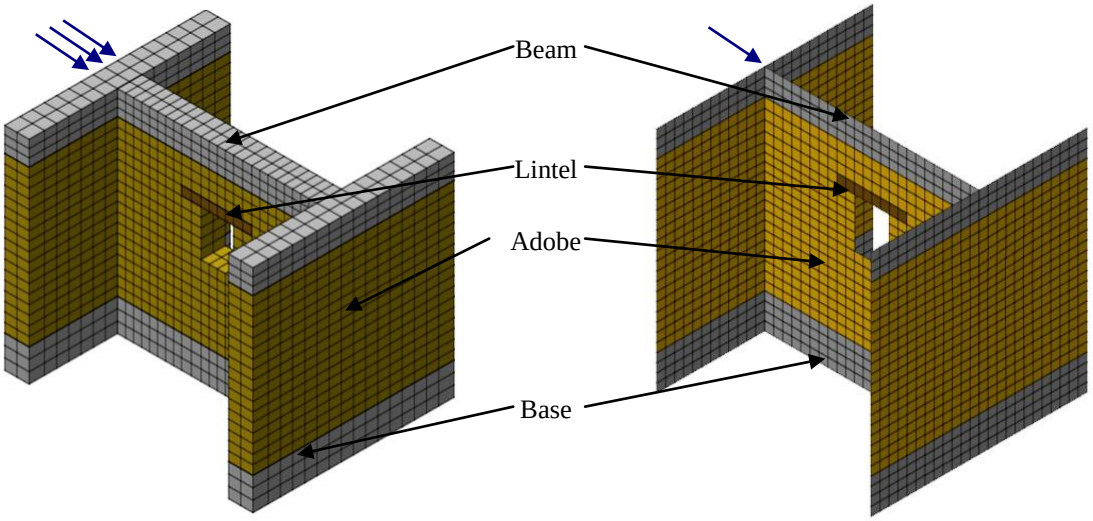

a) Model in Midas FEA (solid elements) b) Model in Midas FEA and Abaqus/Standard (shell elements)

Figure 8.- Numerical models of the tested adobe wall.

The process of loading is as follows: first, the gravity load is applied; then, the horizontal displacement is applied in a given number of steps. In Midas FEA, the lateral displacement is imposed incrementally following the arc-length iterative method in combination with the initial stiffness method. The convergence criterion is controlled through a displacement and energy norm ratio, 0.005 for the former and 0.01 for the later.

In Abaqus/Standard, the top-displacement is imposed following a Newton-Raphson iterative method. An automatic stabilization is selected for the criterion of convergence, with a specified dissipated energy fraction of 0.001 and an adaptive stabilization with maximum ratio to stabilization to strain energy of 0.01.

4.1. Combined crushing-shearing-cracking model

The adobe bricks, the concrete beams and the lintel are modelled using 8-node hexahedron elements and considering elastic and isotropic materials with full integration. The properties adopted for the different materials are shown in Table 1, where E is the elasticity of module, υ is the Poisson's ratio, γ_m is the weight density. In this model, it is assumed that the crack propagation follows the mortar joints, which are modelled with the *combined interface model* with 4 integration points. The adobe blocks are modelled elastically. E is calibrated in order to have a similar initial stiffness as the one obtained from the experimental test.

Table 1.- Elastic material properties.

Adobe			Concrete			Timber		
E (MPa)	υ	γ_m (kN/mm^3)	E (MPa)	υ	γ_m (kN/mm^3)	E (MPa)	υ	γ_m (kN/mm^3)
230	0.2	2.16e-02	22000	0.25	2.35e-02	10000	0.15	6.87e-03

Table 2 shows the material parameters used for the mortar joints to use in the combined crushing-shearing-cracking model. k_n is the normal stiffness modulus, k_t is the shear stiffness modulus, c is the cohesion, φ_o is the frictional angle, ψ is the dilatancy angle, φ_r is the residual friction angle, f_t is the tensile strength, G_{fI} is the fracture energy for Mode I, a and b are factors to evaluate the fracture energy for Mode II (expressed as $G_{II}= a.\sigma+b$), f_c is the compression strength C_s is the shear tension contribution factor, G_{fc} is the compressive fracture energy, and k_p is the peak equivalent plastic relative displacement.

Table 2.- Material properties for the interface model.

Structural						Mode I		Mode II	
k_n (N/mm^3)*	k_t (N/mm^3)*	c (N/mm^2)	φ_o (deg)	Ψ (deg)	φ_r (deg)	f_t (N/mm^2)*	G_{fI} (N/mm)*	a (mm)*	b (N/mm)*
8	3.2	0.05	30	0	30	0.01	0.0008	0	0.01

Compression cap			
f_c (N/mm^2)	C_s	G_{fc} (N/mm)*	k_p (mm)*
0.25	9	0.02	0.09

* The soil mortar properties are taken as lower values than the ones given for adobe blocks (see Table 3), which could be reasonable. Even, the soil mortar properties are calibrated based on the experimental pushover curve and on the real the failure pattern. The hardening/softening curves follow the same shape as the ones specified by Lourenço [8] for clay masonry.

The damaged pattern and deformation at the end of the loading is showed in Figure 9. The crack pattern follows the experimental results: the cracks go from the top left (where the load is applied) to the right bottom of the wall (Figure 3). Since the load applied is monotonic, the FE model cannot capture the X-shape failure. The presence of the two transversal walls prevents the rocking behaviour, representing correctly the testes wall. The maximum displacement reached at the top of the wall is around 6.2 mm, after this the program stopped due to convergence problems.

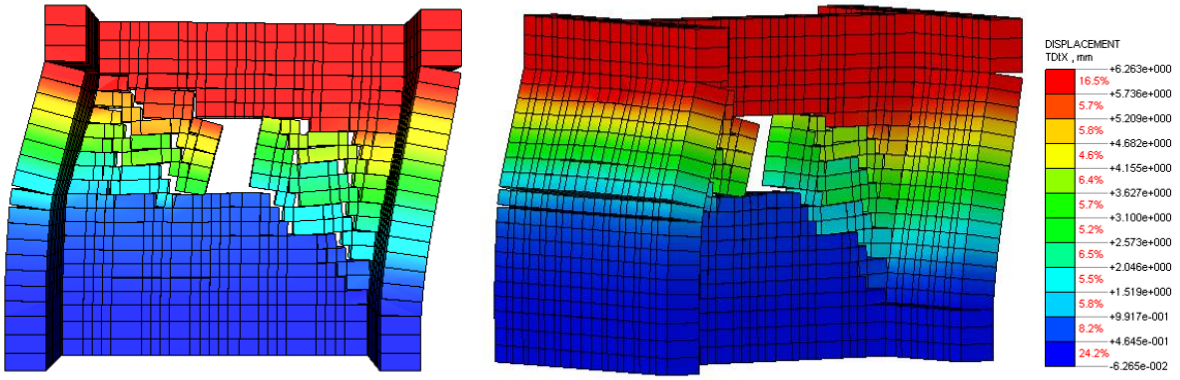

Figure 9.- Deformation pattern of the adobe wall for a lateral displacement considering the *combined interface model*.

4.2. Total strain model

The *total strain model* in Midas FEA makes use of the tension and compression hardening/softening curve of the masonry in terms of stress versus strain (Figure 10). An exponential function is defined for the tension behaviour and a parabolic one (similar to the function given by Lourenço [8]) is given for the compression. Since experimental data for the softening behaviour in tension and compression is not available, the inelastic strain values are assumed based on the ones for clay masonry and calibrated with the pushover curve. The inelastic behaviour in tension and compression are described by the integral of the diagram in Figure 10 (only for the inelastic part). It can be assumed that the adobe material has a brittle behaviour in tension; however, it is believed that rigorous fracture energy should be considered in a more precise model.

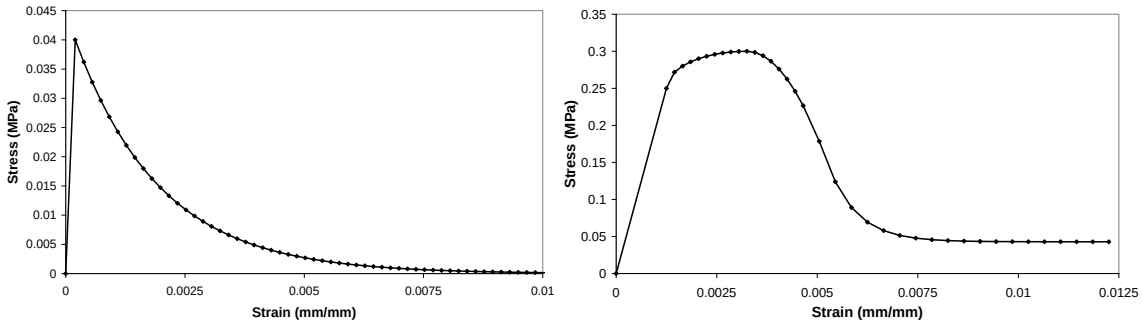

a) Tension b) Compression

Figure 10.- Constitutive laws for the material model in Midas FEA.

It is assumed that adobe masonry behaves as a homogeneous material and cracks are assumed to be smeared. The model is built with rectangular 4 nodes-shell elements. The size of each element is about 100 x 100 mm. The characteristic element length *h* in Midas FEA is given by $\sqrt{2A}$, where *A* is the area of the element.

The elastic module *E* for the complete wall was selected from the adobe masonry tests [15] and then calibrated to have a similar initial stiffness in the pushover curve as the one observed in the test. A compression strength *f'c* close to 0.7 MPa is specified in the literature [15], but the complete definition of the uniaxial behaviour law are not available. *f'c* is obtained from tests on adobe piles (usually 5 adobe blocks placed vertically with earth mortar). The compressive strength of the adobe masonry can be lower than the value obtained from adobe piles tests. Compression tests should be performed on larger specimens in order to have results that can be used in the model considering a homogeneous material (Table 3).

Tensile strength and fracture energy are calibrated in this model using the test results, since no data were found in the literature. Since a fixed crack model is selected, a reduction of the shear stiffness β= 0.1 has been assumed.

The material properties for the concrete and timber are the same as those used in the previous model, presented in section 4.1 (Table 1).

Table 3.- Adobe masonry material properties used for the total strain model.

Elastic				Tension		Compression		
E (N/mm^2)*	υ	γ_m (N/mm^3)	h (mm)	f_t (N/mm^2)*	G_{fl} (N/mm)*	f_c (N/mm^2)*	G_{fc} (N/mm)*	ε_p (mm/mm)*
200	0.2	2.16e-05	140	0.04	0.01	0.3	0.068	0.00325

* calibrated values for adobe masonry.

It is important to remark that properties in Table 2 and Table 3 are different because the former refers to properties for the soil mortar joints; where a tension, compression and shear failure can be located. However, Table 3 refers to properties of masonry walls by using a smeared crack model.

Figure 11 shows the deformation of the wall and Figure 12 shows the cracks pattern of the model (*e.g.* closed, partially open, fully open, etc.), which is in good agreement with the failure pattern observed in the test (Figure 3). Due to problems with the convergence, the maximum displacement reached at the top of the wall is 7.84 mm. As in the previous model, cracks start at the openings corners and progresses diagonally to the wall edges. Figure 13 shows that the maximum strains are reached at the contact zone of the wall with the timber lintel and at the corner openings, this is due to high stress concentration at those zones.

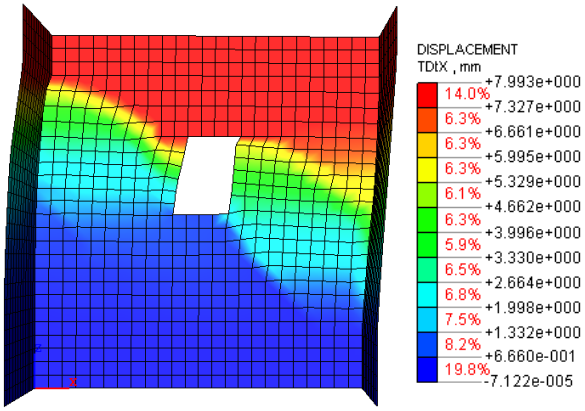

Figure 11.- Deformation of the adobe wall considering the total strain model.

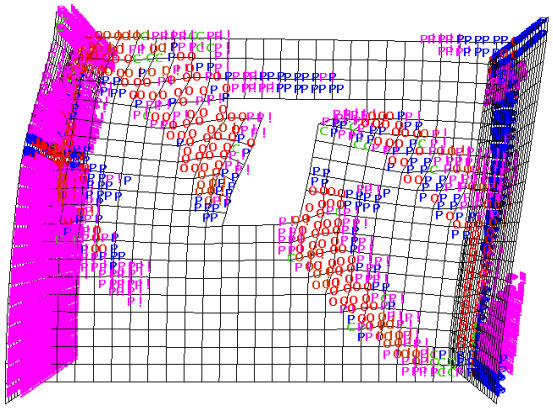

Figure 12.- Crack status
(P: partially open; O: fully open; C: closed).

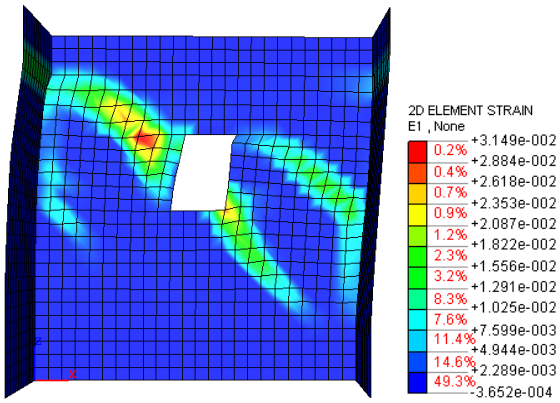

Figure 13.- Element strain at the last step (units in mm/mm).

4.3. Concrete damage plasticity

Similar to the *total strain model*, in the concrete damage plasticity model the inelasticity of the material is represented separately for the tension and compression behaviour laws. In Abaqus/Standard, the material

properties are defined by the stress versus plastic strains constitutive laws (Figure 14). The material properties used in this model are the same as those specified in Table 3.

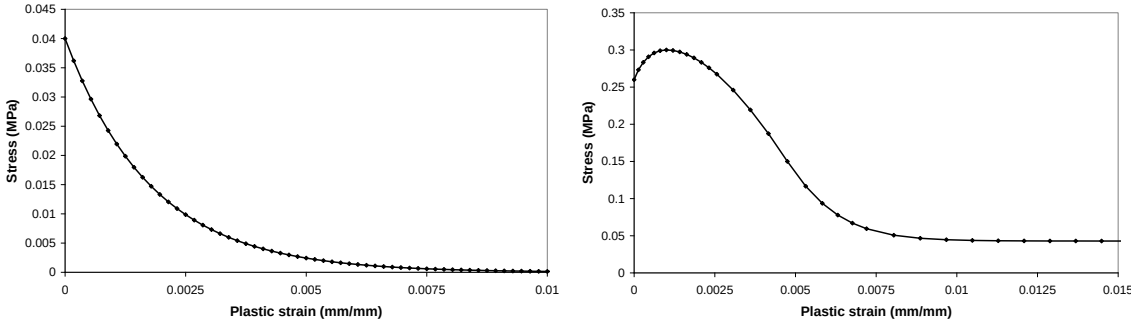

a) Tension b) Compression

Figure 14.- Constitutive laws for the material model in Abaqus/Standard.

Figure 15 shows the wall displacement at the last step of the loading. Figure 16 shows the damage pattern, again the diagonal cracks control the wall behaviour and extend from the opening corners to the wall corners, the red arrows show the tensile plastic strain sand the yellow the compression plastic strains. Figure 16 on the right shows the maximum plastic strains at a displacement of 10 mm at the wall top. It is evident that the high strain values are observed at points in the contact between the timber lintel and the wall and at the opening corners. The inelastic behaviour (fracture energy) in tension and compression are described by the integral of the diagram presented in Figure 14.

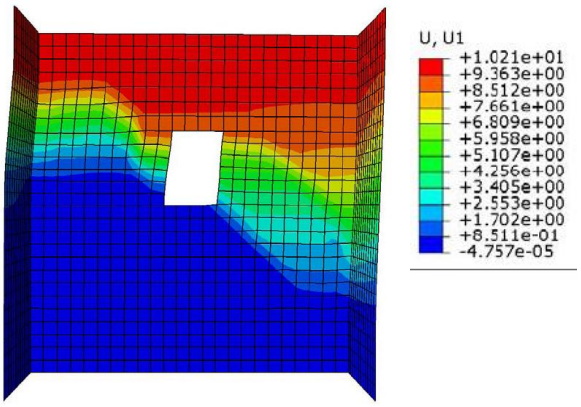

Figure 15.- Displacement of the adobe wall considering the concrete damage plasticity model (units in mm).

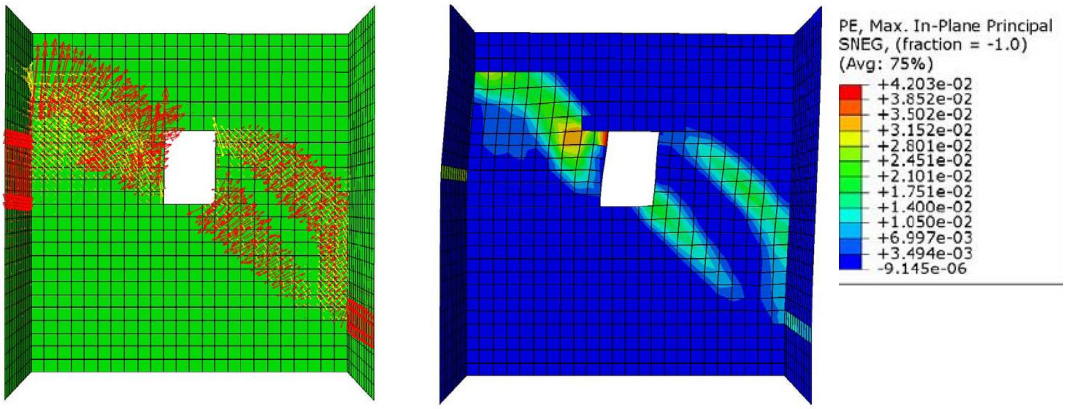

Figure 16.- Maximum plastic strain distribution in Abaqus/Standard (units in mm/mm).

5. ANALYSIS OF THE PUSHOVER CURVES

As it was said before, the ultimate limit state in the adobe wall was considered as 0.52% of drift (10 mm displacement). The maximum force related to this drift was 37.5 kN. All the numerical models reproduced fairly well the general response, the stress distribution and the crack pattern of the wall. Therefore, all the material parameters (elastic and inelastic ones), or at least the ones with larger influence in the masonry response, can be considered correctly calibrated.

The numerical pushover curves represent fairly well the experimental one (Figure 17), especially the first branch, which could be related to the elastic behaviour. When the wall enters in the inelastic range (approximately after 1 mm of top displacement) a dispersion of the numerical pushover curves is observed; however, after 2 mm all the curves match again well the experimental one. It should be noted that this uncertainty is inherent with the nature of the problem and it is found also in the experimental data.

The model with the combined interface law seems to be less ductile than the other ones. This is due to the assumption that the adobe blocks are assumed to be elastic; therefore no tension or compression damage is expected to occur. When the interfaces (mortar) reach the maximum strength in tension or compression, a relative displacement amongst blocks occurs and the pushover curve becomes non-linear. The other numerical models (considering the total strain model and the concrete plasticity model) are more ductile due to the fact that the inelastic properties are distributed all over the wall and not just concentrated at the mortar joins. The first elements that reach the maximum tensile strength are those located at the opening and lintel corners, where stress concentration is expected. Also, horizontal cracks appear at the transversal walls.

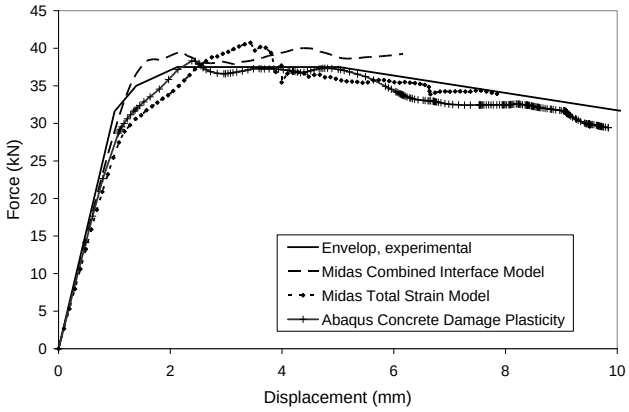

Figure 17.- Pushover curves: experimental results and numerical modelling.

The pushover curve is more sensitive to the variation of tensile strength than to variation of compressive strength. To compare the effect of strength variability, an additional analysis considering *f'c*= 0.4 and 0.7 MPa (corresponding to the values obtained from test on the adobe piles), with a fracture energy proportional to the one considered for *f'c*= 0.3 MPa, is performed and the results obtained are shown in Figure 18.

For the constitutive model used, large compression strength induces an increment in the tensile strength due to biaxial effect. However, after the first diagonal cracks, the pushover curve drops and tends to approach the curve obtained for the nominal strength and experimental results.

Another analysis is done considering no softening in tension (brittle model in Midas FEA). The results, shown in **variation of f'c.** **Figure 19**, reveals a lower wall strength value than the one obtained from the experimental test, which underlines the importance of a correct definition of the fracture energy in tension to properly represent the behaviour of adobe walls.

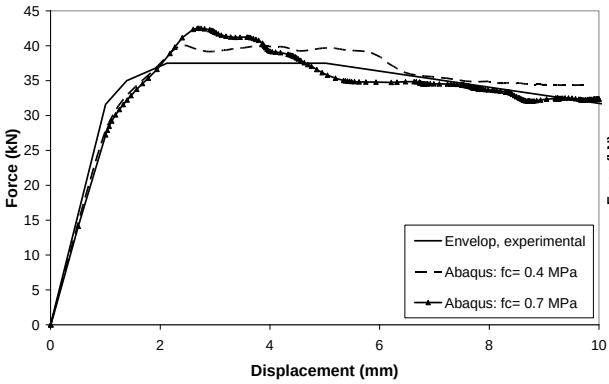

Figure 18.- Pushover curves: variation of f'c.

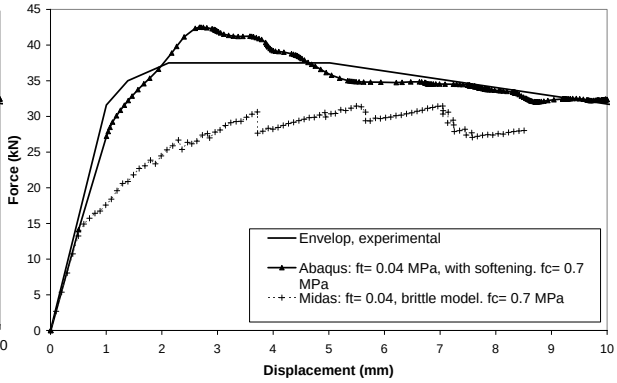

Figure 19.- Pushover curves: Variation of softening in tension.

6. CONCLUSIONS

The material properties used reproduced well the in-plane behaviour of the adobe wall tested. Three numerical models were developed, the first one considers the nonlinearity at the mortar joints, and the other two consider the nonlinearity smeared.

In this work, a variation in the compressive strength was done to see its influence; however, minor effect was observed in the global behaviour of the adobe wall. The results showed that the tensile strength controls the global behaviour. When the maximum tensile strength is reached in one element, stress redistribution occurs and the wall response initiates to be nonlinear. Brittle materials fail due to the progress of internal cracks, inducing a softening behaviour. For the calibration of the softening response of the wall, the constitutive law for tension revealed to be essential to properly reproduce the experimental results.

The lack of experimental data for the evaluation of the hardening/softening behaviour of the adobe material makes difficult to predict numerically the adobe wall behaviour; although, the calibrated material properties represent well the experimental pushover curve. The authors sustained that there is a need of an experimental testing campaign on adobe materials to collect the data necessary to develop and calibrate reliable models.

On-going work includes the analyses for reversal loads and the calibration of the damage parameters, which takes into account residual strains and stiffness recovery (see Figure 7).

7. ACKNOWLEDGEMENTS

The authors express their gratitude to CSP FEA (www.cspfea.net) for providing the program Midas FEA and for the technical support. H. Varum acknowledges the financial support from Fundação para a Ciência e Tecnologia (FCT) through the sabbatical leave grant SFRH/BSAB/939/2009.

8. REFERENCES

[1] Abaqus/Standard 6.9 SIMULIA (2009) Abaqus/CAE Extended Funcionality EF2. Dassault Systemss Corporation. Providence, RI, USA.

[2] Ali, S. S. and Page, A. W. (1988) Finite element model for masonry subjected to concentrated loads. *Journal of Structural Engineering*, ASCE, **114**(8), 1761-1784.

[3] Arya, S. K. and Hegemier, G. A. (1978) On nonlinear response prediction of concrete masonry assemblies. *Proceedings of the North American Masonry Conference*. Masonry Society, Boulder, Colorado, 19.1-19.24.

[4] Blondet, M., Madueño, I., Torrealva, D., Villa-García, G. and Ginocchio, F. (2005) Using industrial materials for the construction of safe adobe houses in seismic areas. *Proceedings of the Earth Build 2005 Conference*, Sydney, Australia.

[5] CUR (1994) Structural masonry: a experimental/numerical basis for practical design rules (in Dutch). Report 171, CUR, Gouda, Netherlands.

[6] Giordano, A., Mele, E. and De Luca, A. (2002) Numerical modelling of masonry structures through different approaches. *Journal of Earthquake Engineering*, ASCE, **24**(8), 1057-1069.

[7] Lofti, H. R. and Shing, P. B. (1994) An interface model applied to fracture of masonry structures. *Journal of Structural Engineering*, ASCE, **120**(1), 63-80.

[8] Lourenço, P.B. (1994) Analysis of masonry structures with interface elements: Theory and applications. Report 03-21-22-0-01, Delft University of Technology, Delft, Netherlands.

[9] Midas FEA v2.9.6 (2009) Nonlinear and detail FE Analysis System for Civil Structures. Midas Information Technology Co. Ltd.

[10] Page, A.W. (1978) Finite element model for masonry. *Journal of Structural Engineering*, ASCE, **104**(8), 1267-1285.

[11] Raijmakers, T.M.J. and Vermeltfoort, A.Th. (1992) Deformation controlled tests in masonry shear walls (in Dutch). Report B-92-1156, TNO, Delft, Netherlands.

[12] Rots, J.G. (1991) Numerical simulation of cracking in structural masonry. *Heron*, **36**(2), 49-63.

[13] Rots, J.G., Berkers, W.G.J. and Heuvel, Van den (1994) Towards fracture mechanics based design rules for movement-joint spacing. *Proceedings of the 10th International Brick and Block Masonry Conference*, University of Calgary, Calgary, Alberta, Canada, 707-717.

[14] Stavridis, A. and Shing, P. B. (2010) Finite element modelling of nonlinear behaviour of masonry-infilled RC frames. *Journal of Structural Engineering*, ASCE, **136**(3), 285-296.

[15] Tarque, N. 2008. Seismic Risk Assessment of Adobe Dwellings. *Master thesis*. European School for Advanced Studies in Reduction of Seismic Risk (ROSE School), University of Pavia, Pavia, Italy. Available at October 2009 from: *http://www.roseschool.it/index.php?option=com_docman&task=doc_download&gid=183&mode=view*

[16] Vermeltfoort, A.Th. and Raijmakers, T.M.J. (1993) Deformation controlled tests in masonry shear walls, Part 2 (in Dutch). Report TUE/BKO/93.08, Eindhoven University of Technology, Eindhoven, Netherlands.

[17] Webster, F. (2008) Earthen Structures: Assessing Seismic Damage, Performance, and Interventions, Terra Literature Review: An Overview of Research in Earthen Architecture Conservation. The Getty Conservation Institute, 69-79. Available at June 2009 from *http://www.getty.edu/conservation/publications/pdf_publications/terra_lit_review.pdf*